EFFECTS OF SOUTHERN CALIFORNIA KELP BEDS ON WAVES

By M. Hany S. Elwany,[1] William C. O'Reilly,[2] Members, ASCE, Robert T. Guza,[3] and Reinhard E. Flick[4]

ABSTRACT: The effect of a *Macrocystis* kelp forest on shoreward propagating surface gravity waves was measured. Observations were made over a 67-day period at four locations around a 350-m-wide kelp bed off Carlsbad, California. Instruments were located directly offshore and onshore of the kelp bed at depths of 13 m and 8 m, respectively, and at control stations at the same depths, but displaced 750 m alongshore, away from the kelp bed. The bathymetry between the offshore and onshore sites was gently sloping and featureless. The measured spectra, significant wave height, mean wave direction at peak frequency, and total radiation stress differed only slightly between the offshore kelp and control stations and were similar at the onshore sites. The similarity of the wave field at the onshore kelp and control sites shows that this typical southern California kelp bed, with an average density of about 10 plants per 100 m^2, does not have a significant effect on waves. These measurements can be used to place upper bounds on drag coefficients in numerical models of the effect of kelp on waves.

INTRODUCTION

The giant kelp *Macrocystis pyrifera* is widespread along the southern California coast (North 1971). The kelp plants grow together, usually in water depths between 8 m and 20 m, forming forests with extensive surface canopies (Deysher and Dean 1986). There are about 15 major kelp beds in southern California, the largest being the 7-km long, 1-km wide Point Loma bed. Bed widths of a few 100 m are more common (North and Jones 1991). Numerical models suggest that surface gravity waves propagating through a kelp bed might undergo various degrees of attenuation, depending on the wave frequency, relative depth, and the kelp plant and forest configurations (Dalrymple et al. 1984; Kobayashi et al. 1993). Although little attenuation might be expected from the typical southern California kelp bed, the hydrodynamics of the flexible plants are complex and the effective drag of kelp on waves is poorly understood. This paper describes unique field measurements, which confirm that a typical southern California kelp bed does not affect shoreward propagating waves.

The experimental strategy was to measure the wave field immediately offshore and onshore of a kelp bed, and to measure the wave field in the same two water depths at a nearby control site. Ideally, the incident wave fields at the offshore kelp bed and offshore control sites would be identical, as would the bathymetry between the offshore and onshore kelp and control sites. In this ideal case, differences between waves at the onshore kelp and control sites could be uniquely ascribed to the effect of the kelp bed.

The field measurements showed that waves were similar not only at the offshore kelp and control sites, but also on the onshore kelp and control stations. However, it is possible that the great similarity between waves at these sites was because of the coincidental compensation of significant kelp-induced wave dampening between the kelp stations and a bathymetrically induced reduction of wave energy between the control stations. However, numerical simulations of waves propagating over the measured bathymetry suggests that the differential effects of wave refraction and diffraction at the kelp and control sites were negligible. This confirms that the test kelp bed did not cause measurable attenuation or changes in the direction of sea and swell waves.

FIELD EXPERIMENT

A kelp bed offshore of Carlsbad, California (Fig. 1) was selected mainly for the location's relatively smooth bathymetry (Fig. 2, measured January 1993). The surface kelp canopy was about 700 m long and 350 m wide. The kelp plant density, estimated from side scan sonar data (Zabloudil et al. 1991), averaged about 10 plants per 100 m^2 and locally exceeded 28 plants per

[1]Res. Assoc., Scripps Instn. of Oceanography, Univ. of Calif., San Diego, La Jolla, CA 92093-0209.
[2]Assoc. Development Engr., Scripps Instn. of Oceanography, Univ. of Calif., San Diego, La Jolla, CA.
[3]Prof., Scripps Instn. of Oceanography, Univ. of Calif., San Diego, La Jolla, CA.
[4]Res. Assoc., Scripps Instn. of Oceanography, Univ. of Calif., San Diego, La Jolla, CA.

Note. Discussion open until September 1, 1995. To extend the closing date one month, a written request must be filed with the ASCE Manager of Journals. The manuscript for this paper was submitted for review and possible publication on May 2, 1994. This paper is part of the ***Journal of Waterway, Port, Coastal, and Ocean Engineering***, Vol. 121, No. 2, March/April, 1995. ©ASCE, ISSN 0733-950X/95/0002-0143–0150/$2.00 + $.25 per page. Paper No. 8345.

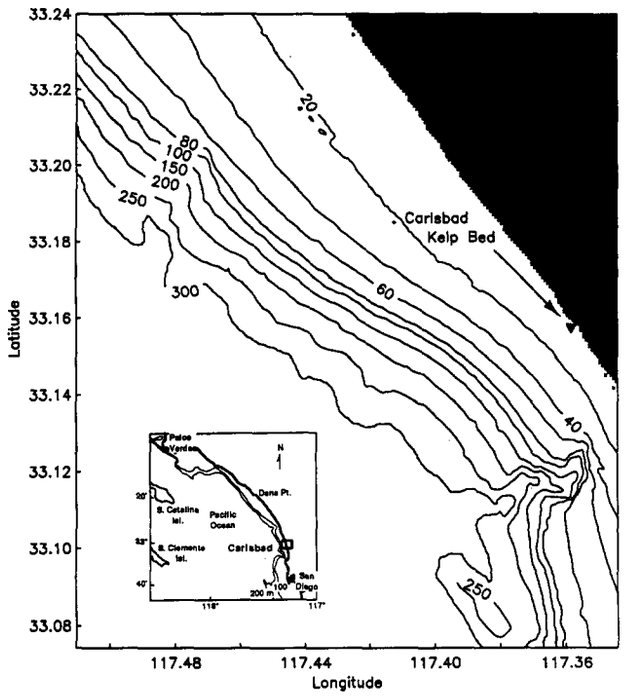

FIG. 1. Continental Shelf Bathymetry Contours (*m*) Offshore of Carlsbad

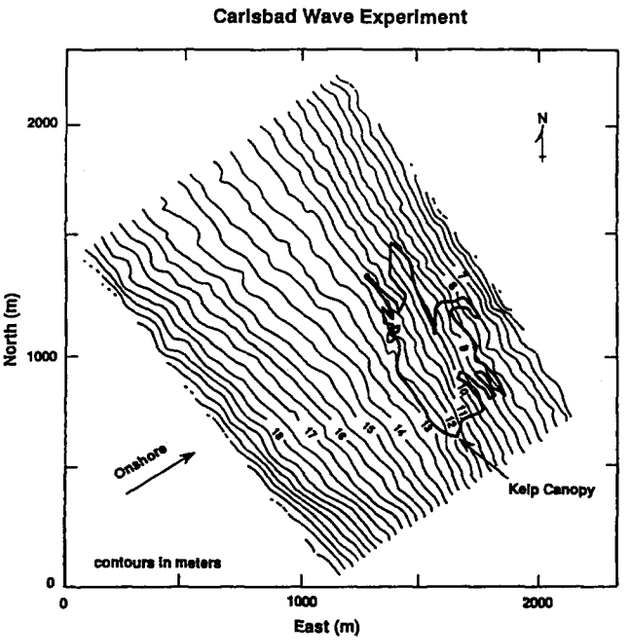

FIG. 2. Bathymetry and Kelp Canopy Coverage at Carlsbad Kelp Bed

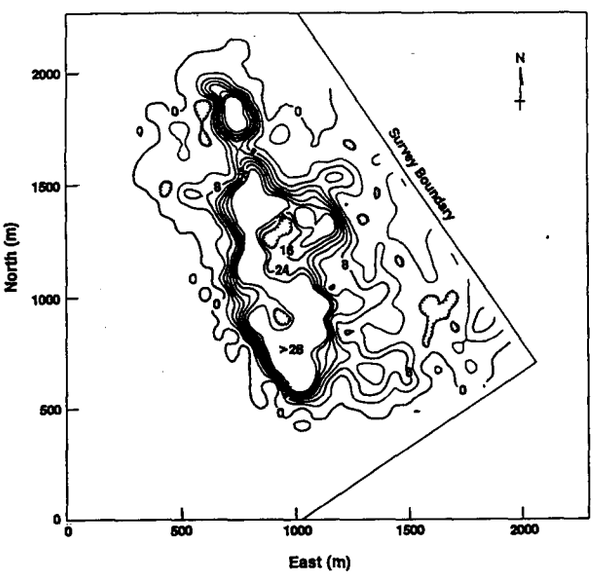

FIG. 3. Kelp Density (Number of Plants per 100 m^2) at Carlsbad Kelp Bed

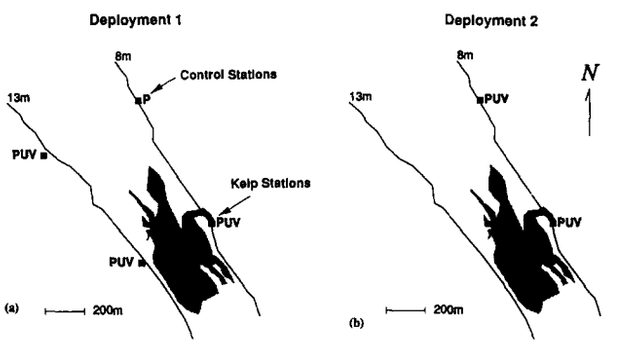

FIG. 4. Instrument Positions at Carlsbad Test Site, 8-m and 13-m Depth Contours Are Indicated

100 m^2 (Fig. 3). The bottom substrate was a mix of sand and sandstone with low relief, typically between 20 cm and 50 cm. Rocks along the onshore parts of the kelp bed protruded as much as 90 cm above the bottom.

To measure effects of the kelp bed, concurrent wave measurements were made immediately seaward (13 m deep) and shoreward (8 m deep) of the bed, and at control sites located 750 m north of the kelp stations and about 300 m north of the kelp bed boundary (Fig. 4). Extensive numerical simulations of waves propagating across the continental shelf (Fig. 1), following O'Reilly and Guza (1993), suggested that the wave field at the 13-m depth control and kelp sites would be very similar, as was subsequently observed.

InterOcean Systems S4DW and S4 wave gauges, (Trageser and Elwany 1990) were deployed. The S4DW gauge measured water pressure (P) and the two horizontal components of wave-induced orbital velocity (U and V), and is referred to as a *PUV* gauge in Fig. 4. Bulk directional

properties of the wave field, such as the mean wave direction and the total (frequency integrated) radiation stress (S_{xy}), were estimated from *PUV* gauge data. The S4 gauge measured pressure (*P* in Fig. 4) from which the wave energy could be obtained, but not the wave directional properties. All instruments were mounted on pipes about 1 m above the sea floor, and sampled daily for approximately 2 hr and 16 min at 1 Hz.

The instruments were deployed for 31 days between February 13 and March 20, 1993 (deployment 1), and for 36 days between April 14 and May 20, 1993 (deployment 2). During the first deployment, *PUV* gauges were placed at the 13-m kelp and control sites and at the 8-m kelp site, and a *P* gauge was located at the 8-m control station (Fig. 4). *PUV* gauges were located at both 8-m sites for the second deployment.

DATA ANALYSIS

Wave energy spectra and directional properties were estimated by first dividing each 2.3-hr record into eight 17-min subrecords. Each subrecord was linearly detrended, tapered with a triangle Parzen window and fast Fourier transformed. The Fourier coefficients were surface-corrected using linear wave theory, and combined to form standard [e.g., Nagata (1964)] auto and cross spectra. The spectra were frequency-merged into 0.01-Hz-wide frequency intervals and averaged over the 17-min subrecords to yield smoothed spectra with 160 degrees of freedom (dof). The directional distribution of wave energy $E(f, \theta)$, in which θ is the wave propagation direction relative to onshore, can be expressed as a Fourier series

$$E(f, \theta) = \frac{a_0(f)}{2\pi}\left[1 + 2\sum_{n=1}^{\infty} a_n(f)\cos(n\theta) + b_n(f)\sin(n\theta)\right] \tag{1}$$

The wave energy a_0 and the first four Fourier coefficients of the directional distribution (a_1, b_1, a_2, b_2) at frequency f were calculated from the measured *PUV* cross spectra.

Wave-induced pressure fluctuations attenuate with depth. Near the surface, higher-frequency waves attenuate more rapidly than lower-frequency waves. Nonlinear effects are accentuated at depths that are large relative to a surface wavelength, and measurements taken by near-bottom pressure sensors and interpreted using linear theory are effectively frequency-limited (Herbers and Guza 1991). The pressure gauges deployed at depths of 8 m and 13 m had estimated cutoff frequencies of 0.30 Hz and 0.23 Hz, respectively. Instrumental noise in the current meter-limited wave direction estimates frequencies below 0.20 Hz and 0.23 Hz at depths of 13 m and 8 m, respectively. Wave information at frequencies above the cutoff was not considered in detail, but the vast majority of wave energy incident on the kelp bed was at frequencies below 0.20 Hz.

Nondirectional wave parameters used to compare wave conditions at different measurement locations included the frequency spectrum $E(f)$ and the significant wave height $H_s = 4(\int E(f)df)^{1/2}$. Confidence limits on H_s are a function of the total degrees of freedom (tdof) (Donelan and Pierson 1983), and

$$\text{tdof} \approx \text{dof}\,\frac{\left[\sum E(f)\right]^2}{\sum [E(f)]^2}, \tag{2}$$

where Σ = sum over all frequencies. The tdof varied between 400 and 2,000 with day-to-day changes in $E(f)$. The greatest uncertainties occurred when $E(f)$ was relatively narrow. The corresponding 90% confidence limits on H_s ranged approximately between 4% and 9%.

Two directional parameters were calculated: the mean wave direction $\bar{\theta}$, and S_{xy}, the component of the radiation stress tensor that drives longshore currents and sand transport (Longuet-Higgins 1970). For each 0.01-Hz-wide frequency interval,

$$\bar{\theta}(f) = \tan^{-1}\left[\frac{b_1(f)}{a_1(f)}\right] \tag{3}$$

where a_1, b_1 = first two Fourier coefficients of the directional distribution. The standard deviation of $\bar{\theta}$ is (Kuik et al. 1988)

$$sd(\bar{\theta}(f)) = \frac{\sqrt{(1 - m_2(f))/(2m_1(f)^2)}}{\sqrt{\text{dof}}} \tag{4}$$

where $m_1(f) = \sqrt{a_1^2(f) + b_1^2(f)}$ and $m_2(f) = \sqrt{a_2^2(f) + b_2^2(f)}$. Because a_1, b_1, a_2, and b_2 depend on the shape of the directional distribution, the confidence limits on $\bar{\theta}$ varied, and 90% levels (equal to ± 1.67 times the standard deviation) were between about 2° and 5°. S_{xy} is given by (Longuet-Higgins 1970)

$$S_{xy} = \frac{1}{2} \sum_f E(f) \frac{C_g(f)}{C(f)} b_2(f) \Delta f \tag{5}$$

where C_g and C = group and phase velocities, respectively. The standard deviations of the S_{xy} estimates were approximated after Borgman et al. (1982)

$$sd(S_{xy}) = a_0 \sqrt{(1 - a_2^2 + b_2^2)(4 \text{ tdof})^{-1}} \tag{6}$$

where a_0, a_2^2, and b_2^2 were integrated over the entire frequency range, 0.05–0.20 Hz at 13 m, and 0.05–0.23 Hz at 8 m.

EXPERIMENT RESULTS

The significant wave height H_s, mean wave direction at the peak wave period $\bar{\theta}$ at T_p, and the total radiation stress S_{xy} are typically used to design coastal structures and estimate alongshore sediment transport [e.g., *Shore* (1984)]. A large impact of the kelp bed on the incident wave field would have been apparent in these bulk parameters. More subtle potential effects of the kelp bed were examined by comparing the frequency distributions of wave energy and wave direction at the kelp and control sites.

The wide range of wave conditions measured during the 67-day-long experiment are shown in Fig. 5. H_s ranged between about 50 cm and 190 cm, T_p between 6 s and 19 s, and $\bar{\theta}$ at T_p differed by as much as 30° from the normal incidence (230°), as shown in Fig. 5(a).

Bulk Wave Parameters

Daily estimates of H_s during deployment 1 are compared at the 13-m and 8-m sites in Fig. 6. The dashed line represents equality of the kelp and control measurements. The 90% confidence limits are shown for the control site estimates, and are very similar for the kelp site data. The observed differences between the kelp and control estimates of H_s were comparable with the statistical fluctuations expected in a spatially homogeneous wave field.

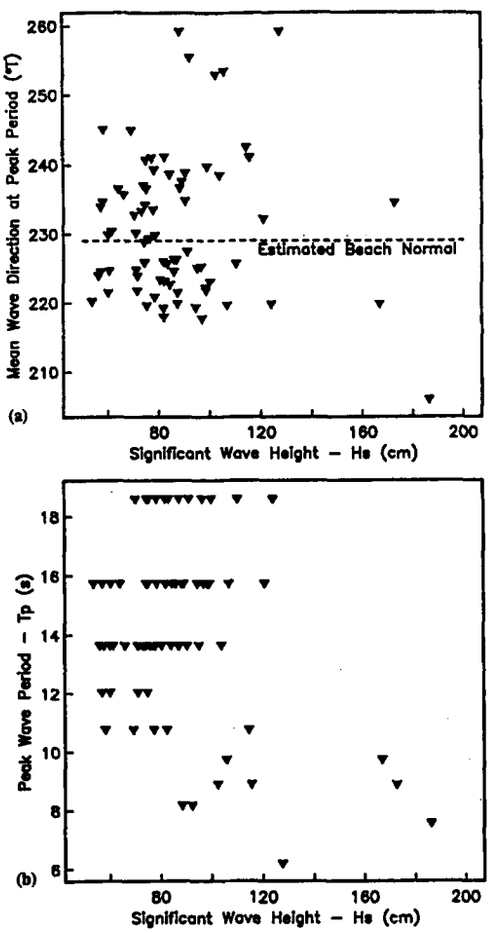

FIG. 5. Range of Wave Conditions Measured (Daily) at 8-m Kelp Station

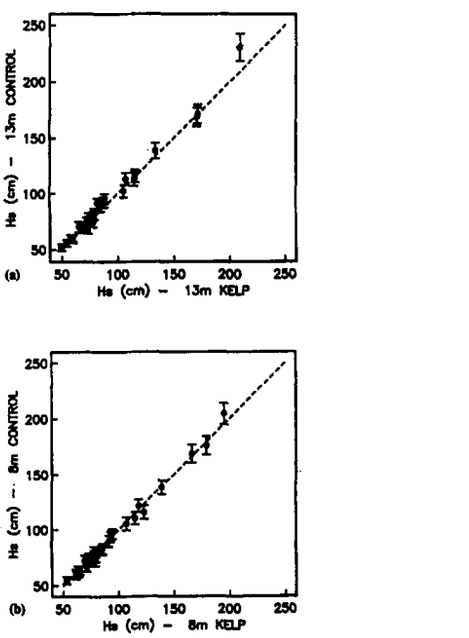

FIG. 6. (a) Significant Wave Heights at 13-m Stations; (b) at 8-m Stations during Deployment 1

Similar comparisons for $\bar{\theta}$ at T_p indicated a small (3–5°) but statistically significant difference between the mean wave directions at the two 13-m stations [Fig. 7(a)], but not at the 8-m stations onshore of the kelp bed [Fig. 7(b)] (90% confidence limits are shown). Numerical simulations of waves propagating across the shelf (Fig. 1) suggest only very small bathymetrically induced differences in wave direction, and the measured angular difference was probably due to a compass error. Because a *PUV* instrument is needed to calculate $\bar{\theta}$ at T_p, these estimates for the 13-m and 8-m stations were from different deployment periods (Fig. 4).

Estimates of S_{xy} fell slightly above the line of equality at the depth of 13 m during deployment 1 [Fig. 8(a)], consistent with the small difference in the approach direction in $\bar{\theta}$ at T_p (Fig. 7). A similar comparison at the 8-m stations during deployment 2 [Fig. 8(b)] shows no significant differences in S_{xy} (90% confidence limits are shown here).

Frequency-Dependent Wave Parameters

It is widely accepted that the energy dissipated by waves propagating through a kelp bed varies with wave frequency [Kobayashi et al. (1993) and references therein]. Low-frequency waves are less dampened than the shorter, high-frequency waves. Because frequency-dependent wave energy dissipation by the kelp could be masked by the frequency integration used to derive the bulk parameters, the frequency-dependent mean wave directions $\bar{\theta}(f)$ and the wave energy $E(f)$ were also compared. To simplify the data presentation and interpretation, daily estimates of $\bar{\theta}(f)$ and $E(f)$ were averaged over each deployment, forming the deployment mean quantities $\langle\bar{\theta}(f)\rangle$ and $\langle E(f)\rangle$.

The energy spectra $\langle E(f)\rangle$ averaged over deployment 1 show slightly greater wave energy (5–10%) at the 13-m control station than at the 13-m kelp station at wave frequencies higher than 0.10 Hz [Fig. 9(a)]. However, at the 8-m stations the spectra were nearly identical over the same 31-day period [Fig. 9(b)]. Deployment 1-averaged mean directions as a function of frequency, $\langle\bar{\theta}(f)\rangle$, at the 13-m stations indicate that the 3–5° directional difference in $\bar{\theta}$ at T_p [Fig. 7(a)] was present over all measured wave frequencies (not shown). This is consistent with the angular difference being caused by compass bias, since a constant directional rotation of all frequencies is physically unlikely. During deployment 2, $\langle E(f)\rangle$ at the 8-m kelp station was slightly (5–10%) larger than $\langle E(f)\rangle$ at the 8-m control station, at wave frequencies between 0.12 and 0.16 Hz [Fig. 10(a)]. The deployment averaged $\langle\bar{\theta}(f)\rangle$ at the 8-m depth differed by only 1–2° [Fig. 10(b)].

The measured differences between wave fields at the kelp and control stations approached the instrument accuracies. Compass errors of a few degrees are typical for directional instruments, and pressure sensor calibration uncertainty generally produces errors of a few percent in wave energy. Alternatively, if we assume the present measurements were error-free, the differences in the incident wave field at the 13-m kelp and control stations were about 5–10% in $E(f)$ and 5° in $\bar{\theta}(f)$. If real, this inhomogeneity places lower bounds on the sizes of wave energy and wave direction differences at the 8-m stations that could be ascribed to the kelp; i.e., differences at the 8-m sites must be larger than those at the 13-m sites to conclusively show a kelp effect. In fact, the differences at 8-m depth are slightly smaller than those observed at the 13-m depth sites (Fig. 9).

There was no measurable difference of wave energy or direction between the 8-m kelp and control stations for wave periods of 3–20 s, given the accuracy of the instruments and the possible small differences in incident wave conditions between the 13-m kelp and control sites. The definition of "measurable" in this case is 5–10% in $E(f)$ and 3–5° in wave direction.

NUMERICAL WAVE MODEL

The conclusion that the kelp bed did not measurably affect waves is based on the assumption that the bathymetry between the 13-m and 8-m kelp stations was similar to that between the

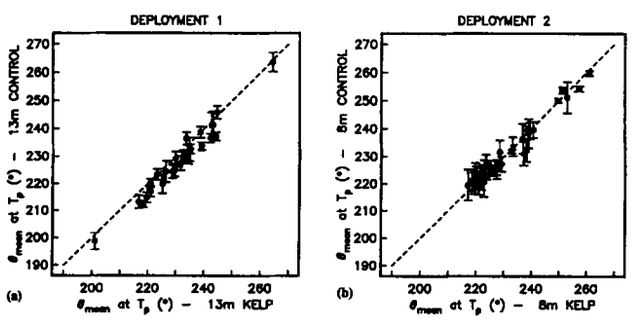

FIG. 7. (a) Mean Wave Directions at Peak Wave Period at 13-m Stations; (b) at 8-m Stations

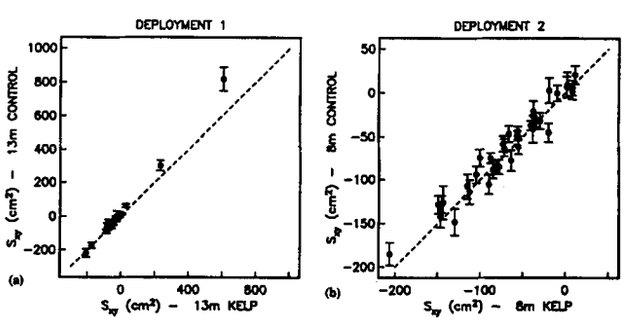

FIG. 8. (a) Total Radiation Stress at 13-m Stations; (b) at 8-m Stations, right

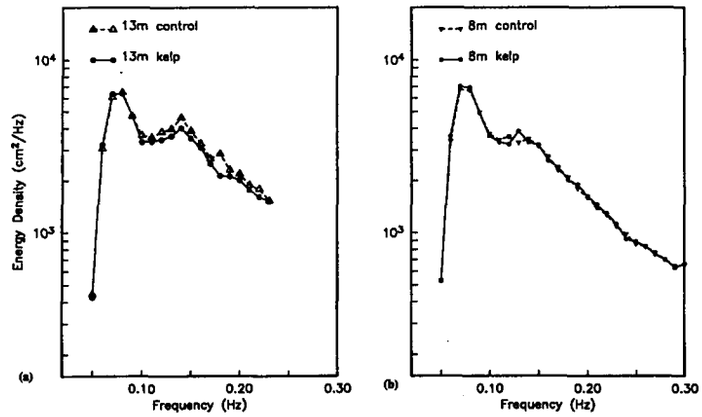

FIG. 9. Averaged Spectra of Sea Surface Elevation during Deployment 1

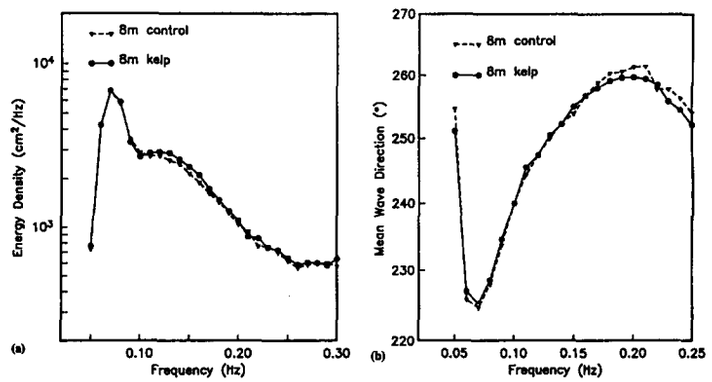

FIG. 10. (a) Averaged Sea Surface Elevation Spectra; (b) Mean Wave Direction at 8-m Stations during Deployment 2

13-m and 8-m control stations, in the sense that bathymetry-induced differences between wave fields at the 8-m kelp and control sites were negligible. It is possible, albeit unlikely, that this assumption is false and the great similarity between waves at the 8-m sites was because of the coincidental compensation of significant kelp-induced wave dampening at the kelp site and a bathymetrically induced reduction of wave energy at the control site. A numerical model was used to show that bathymetry did not introduce such effects, and that the kelp-induced dampening was indeed small.

Wave propagation between the 13-m and 8-m depth sites was simulated over recently measured bathymetry (Fig. 2) with a numerical model of the refraction, diffraction, and shoaling of monochromatic, unidirectional incident waves (Kirby 1986). Results for individual incident wave frequencies and directions were combined to model the transformation of directional wave spectra (Izumiya and Horikawa 1987). The purpose of the simulations was to isolate the effects of the slightly irregular bathymetry while neglecting any kelp influences.

To characterize typical wave spectrum transformations between 13-m and 8-m depths, simulations were performed in 0.01-Hz-wide frequency intervals in the 0.10–0.20-Hz local sea band. For each frequency interval, a unimodal wave spectrum with a full width at half maximum power of 30° was used to initialize the model. The peak direction of this spectrum was varied from 210° to 260°, corresponding with the range of typical mean wave directions (Fig. 5). Each input spectrum was numerically transformed from the 13-m contour to the 8-m instrument stations. The ratio of wave energy at the two 8-m stations ($E_{\text{kelp}}/E_{\text{control}}$) differed from unity by less than 0.1 (Fig. 11). Alongshore variability in the bathymetry between the 13-m and 8-m depth near the control and kelp sites caused only small differences in the energies at the 8-m kelp and control sites.

The model wave spectra chosen to initialize these simulations at the 13-m contour represent spatially homogeneous spectra with a typical directional distribution. The results in Fig. 11 do not account for the small longshore variability in the wave field measured at the 13-m stations or for deviations from a hypothetical directional distribution. Estimates of the combined effects of irregular bathymetry, more realistic directional distributions, and possible alongshore variations in the kelp and control wave fields at the 13-m depth sites are now shown.

The energy in each spectrum measured at the 13-m depth sites was summed into three broad bands: 0.05–0.10 Hz, 0.10–0.15 Hz, and 0.15–0.20 Hz. At the 8-m depth sites, where wave-

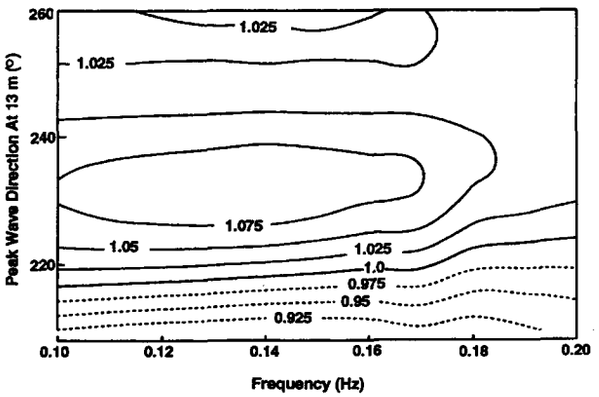

FIG. 11. Contours Predicted Ratio $E(f)_{kelp}/E(f)_{control}$ at 8-m Depth as Function of Wave Frequency and Mean Wave Direction at 13-m Isobath (Solid and Dashed Lines Indicate Ratios Greater and Less than 1.0, Respectively)

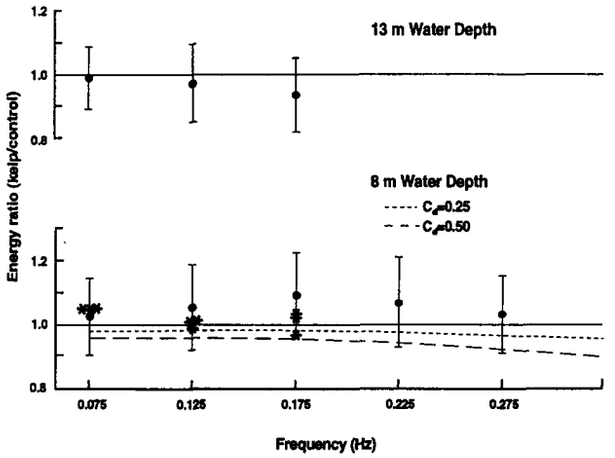

FIG. 12. Average Wave Energy Ratios during Deployment 1 in 0.05-Hz-Wide Frequency Bands (Solid Circles Are Mean Observed Ratios and Vertical Bars Are One Standard Deviation)

induced pressure fluctuations at the sea floor were less attenuated, accurate measurements extended to higher frequency and two additional frequency bands were included: 0.20–0.25 Hz and 0.025–0.30 Hz. The ratio of the energy between the kelp and control stations at the 8-m depth and the 13-m depth sites was calculated for each broad frequency band from each daily measurement. These individual ratios were then averaged over all observations, and were found to differ only slightly from 1.0. In all three frequency bands, the mean energy at the 13-m control station was, on an average, less than 10% greater than the mean energy at the 13-m kelp station (Fig. 12, upper part). In the 8-m water depth, the ratio was similarly close to 1.0 (upper part of Fig. 12).

The frequency-directional spectrum at the 13-m depth sites was calculated for each record with the maximum entropy method (Lygre and Krogstad 1986). The fidelity of these estimates is limited by instrument inaccuracies and the fundamentally low resolution of a *PUV* system. Nonetheless, they do reflect the variety of directional distributions encountered during the study.

The estimated directional distributions and the measured bathymetry were used in conjunction with the Kirby (1986) wave propagation model to predict energy ratios in the 8-m water depth. The predicted ratios were averaged over the same set of incident wave spectra as the observed ratios. If the bathymetry had no alongshore variation and the incident wave field was spatially homogeneous in 13-m water depth, the predicted ratios would equal unity.

The asterisks (three for each of the three lowest frequency bands) in Fig. 12 (lower) indicate the energy ratios predicted at the 8-m depth using three slightly different estimates of the frequency-directional distribution at the 13-m depth. The three asterisks at each central frequency are slightly offset for clarity. One estimate is based on a spatially inhomogeneous wave field, which mimics the measured 3–5° average difference in wave propagation angles [Fig. 7(a)] and small differences in energy observed at the 13-m depth [Fig. 9(a)]. In the other two estimates, these differences were assumed to be a result of instrumental errors, and the wave field at the 13-m depth was modeled as two slightly different versions of a homogeneous wave field.

The predicted energy ratios at the 8-m depth (asterisks in the lower part of Fig. 12) deviated by less than 0.1 from the observed ratios and from unity. Alongshore inhomogeneity in the bathymetry between 13-m and 8-m depths, and in $E(f, \theta)$ at the 13-m depth, were unimportant to wave energy at 8-m depth.

The numerical model neglected any possible effects of kelp. The agreement between the model predicted and observed ratios (lower part of Fig. 12) quantitatively supports the conclusion that the kelp had no measurable effect on the waves. Although the predictions included only frequencies below 0.2 Hz (the maximum frequency for which frequency-directional spectra could be estimated at the 13-m depth), the observed near-unity ratio values observed at the 8-m depth extend to 0.3 Hz (Fig. 12, lower part). This suggests that the entire frequency range from long swell to high-frequency seas was unaffected by the kelp bed.

COMMENT

State-of-the-art numerical models cannot accurately predict the effect of kelp on waves, because the effective drag exerted by individual or grouped kelp plants is unknown (Dalrymple et al. 1984; Kobayashi et al. 1993). Kelp plants have apparently evolved a hydrodynamically streamlined form, which enables them to comply with the flow, both at the small scale of individual fronds and at the larger scale of the plant stalk that spans the water column. There

are no models that accurately estimate the net drag of these hydrodynamically complex plant structures; so, wave propagation models cannot be used for accurate predictions as yet. "Extensive field data will be required to better predict the drag coefficient," Kobayashi et al. (1993).

The observations at the Carlsbad, California kelp bed are the most extensive available and can be used to estimate a rough upper bound on the unknown drag parameters. The dashed lines in Fig. 12 correspond with the predicted 8-m depth energy ratio, in which the deviation from unity is due to the frequency-dependent dampening by kelp, predicted by Dalrymple et al. (1984), using C_d values of 0.25 and 0.5. The depth was taken as 10 m, and parameters such as the kelp bed width were chosen to represent the Carlsbad test site. C_d must be less than roughly 0.5, or wave dampening would have been apparent in the observations. Only an upper bound can be estimated for C_d, because any C_d value less than 0.5 would also be in agreement with the observations. For cases like the Carlsbad one, the small kelp-induced wave dampening may as well be ignored. However, the upper limit estimate of C_d may be relevant when modeling the possible dampening effects of much wider kelp beds.

SUMMARY

The effect of the 350-m-wide Carlsbad kelp bed on surface waves was not detectable. The measured differences between waves at onshore kelp and control stations did not exceed differences expected from other causes. The measured differences in wave energy, the modeled differences owing to alongshore variations in the bathymetry and incident wave field, and the accuracy of the instruments themselves were of similar magnitude (5–10% in wave energy and 3–5° in direction).

ACKNOWLEDGMENTS

The writers gratefully acknowledge the support from the Southern California Edison Company (SCE). We thank Robert Grove and Frank Malone of SCE for their support, which made it possible to perform this experiment before the end of the 1993 storm season. W. A. Boyd ably handled all aspects of data acquisition, including instrument preparation and deployment. We also thank Karel Zabloudil, Neil Marshall, Timothy Norall, and Kyle Marshall for assistance in site selection, conducting the bathymetry and help density surveys, and helping with field work. We are indebted to Dr. Choule Sonu for helpful comments that improved the study.

APPENDIX. REFERENCES

Borgman, L. E., Hagan, R. L., and Kuik, T. (1982). "Statistical precision of directional spectrum estimation with data from a tilt-and-roll buoy." *Topics in Ocean Physics*, A. R. Malanotte-Rizzoli, Noord, Holland, 418–438.

Dalrymple, R. A., Kirby, J. T., and Hwang, P. A. (1984). "Wave diffraction due to areas of energy dissipation." *J. Wtrwy., Port, Coast., and Oc. Engrg.*, ASCE, 110(1), 67–79.

Deysher, L. E., and Dean, T. A. (1986). "In situ recruitment of sporophytes of the giant kelp, *Macrocystis pyrifera (L.)* C. A. Agardh: effects of physical factors." *J. Experimental Marine Biology and Ecology*, 103(1–3), 41–63.

Donelan, M., and Pierson, W. J. (1983). "The sampling variability of estimates of spectra of wind-generated gravity waves." *J. Geophysical Res.*, 88(7), 4381–4392.

Herbers, T. H. C., and Guza, R. T. (1991). "Wind wave nonlinearity observed at the sea floor, Part I: forced wave energy." *J. Physical Oceanography*, 21(12), 1740–1761.

Izumiya, T., and Horikawa, K. (1987). "On the transformation of directional waves under combined refraction and diffraction." *Coast. Engrg. in Japan*, Tokyo, Japan, 30(1), 49–65.

Kirby, J. T. (1986). "Higher-order approximations in the parabolic equation method for water waves." *J. Geophysical Res.*, 91(C1), 933–952.

Kobayashi, N., Raichle, A. W., and Asano, T. (1993). "Wave attenuation by vegetation." *J. Wtrwy., Port, Coast., and Oc. Engrg.*, ASCE, 119(1), 30–48.

Kuik, A. J., van Vledder, G. P., and Holthuijsen, L. H. (1988). "A method for routine analysis of pitch-and-roll buoy data." *J. Physical Oceanography*, 18(7), 1020–1034.

Longuet-Higgins, M. S. (1970). "Longshore currents generated by obliquely incident sea waves." *J. Geophysical Res.*, 75(33), 6778–6789.

Lygre, A., and Krogstad, H. E. (1986). "Maximum entropy estimation of the directional distribution in ocean wave spectra." *J. Physical Oceanography*, 16(12), 2052–2060.

Nagata, Y. (1964). "The statistical properties of orbital wave motions and their application for the measurement of directional wave spectra." *J. Oceanographical Soc. of Japan*, Tokyo, Japan, 19(4), 169–181.

North, W. J. (1971). *The biology of giant kelp beds (Macrocystis) in California*, Verlag, Von J. Cramer, Lehre.

North, W. J., and Jones, G. J. (1991). "The kelp beds of San Diego and Orange Counties." *Rep.; 2 Appendixes*, San Diego Regional Water Quality Board, San Diego, Calif.

O'Reilly, W. C., and Guza, R. T. (1993). "A comparison of spectral wave models in the Southern California Bight." *Coast. Engrg.*, 19(3), 263–282.

Trageser, M. A., and Elwany, H. M. S. (1990). "The S4DW, an integrated solution to directional wave measurements." *Proc., Marine Instrumentation '90*, West Star Productions, Spring Valley, Calif., 118–140.

"*Shore protection manual*," 4th Ed. (1984). U.S. Army Corps of Engrs., W Experiment Station, Vicksburg, Miss.

Zabloudil, K. F., Reitzel, J. S., Schroeter, S. C., Dixon, J. D., Dean, T. A., and Norall, T. L. (1991). "Sonar mapping of giant kelp density and distribution, coastal zone '91." *Proc., 7th Symp. on Coast. and Oc. Mgmt.*, ASCE, New York, N.Y.